

Deformation of λ -Phage DNA Molecules in an Elongational Flow Field

NAOKI SASAKI,^{1,*} ICHIRO HAYAKAWA,¹ KUNIO HIKICHI,¹ and EDWARD D. T. ATKINS²

¹Division of Biological Sciences, Graduate School of Science, Hokkaido University, Sapporo 060, Japan;

²H. H. Wills Physics Laboratory, University of Bristol, Tyndall Avenue, Bristol BS8 1TL, United Kingdom

SYNOPSIS

The response of λ -phage DNA molecules to a well-defined elongational flow field generated by a Taylor four-roller mill was investigated by observing the flow birefringence, Δn . Δn in the center of the four rollers, near the stagnation point, was localized at the mill exit symmetry plane. The intensity gradually increased from the off-symmetrical plane to the center of the mill, and at the exit symmetrical plane, the intensity was maximum. Δn also gradually increases with the strain rate, $\dot{\epsilon}$. These observations indicate that DNA molecules in the solution would be free draining in nature. From the decay of Δn at each point in the mill after a sudden stop of the mill operation at 24 s^{-1} , the rotational diffusion coefficient of molecules, D_r , at each point in the mill space was estimated, where the relaxation time of the decay of Δn was considered to be related to the molecular disorienting process. It is concluded that at 24 s^{-1} λ -phage DNA molecular coils near the stagnation point, which was assumed to be a prolate spheroid as a whole, was so deformed that the aspect ratio p ($=b/a \leq 1$, where a and b are, respectively, the longer and shorter axes) would be $\frac{1}{12}$ of that of the DNA molecule which has just entered the mill space. This result suggests that there is a possibility for the DNA molecule to be in a stretched conformation at a higher strain rate. © 1996 John Wiley & Sons, Inc.

INTRODUCTION

The static and dynamic properties of DNA are of fundamental importance in biology. The stiffness of DNA determines both its persistence length and its dynamic properties, as well as the strain energy stored in highly distorted DNA. At the same time, since phage DNA such as λ -phage DNA has a large molecular weight with monodisperse distribution, it is used as a model system for visualizing single-polymer molecules and testing theories about the dynamic motion of polymer molecules.^{1,2}

It has been well established that flexible polymers manifest a conformational transition in a well-defined elongational flow field: a coil-stretch transition.³⁻⁶ In a stretched state, a polymer molecule is considered to be in an almost fully extended conformation, which has been deduced from molecular

scission by an elongational flow field. On the other hand, light-scattering investigation of flexible polymers in conjunction with elongational flow experiments revealed that, even in the stretched state, the radius of gyration of the polymer molecule was only twice that in the quiescent state.⁷ If the overall structure of a polymer can be considered as an ellipsoid, this result indicates that the aspect ratio p ($=b/a$, where a and b are, respectively, the longer and shorter axes of the prolate spheroid) in the flow field decreases to be about $\frac{1}{6}$ of the ratio of the unperturbed molecule.⁸

Previous elongational flow works on DNA molecules revealed that the scission of molecules in an elongational flow field halves the molecular weight.^{9,10} This suggests that DNA molecules in a flow field of high strain rate would be in an almost fully extended conformation.

The purpose of the present work was to estimate the degree of extension of a molecule in a flow field. For this, we studied the response of DNA molecules in a solution to the well-defined elongational flow

* To whom correspondence should be addressed.

field which was generated by the Taylor four-roller mill system. We used λ -phage DNA, which has a monodisperse molecular weight distribution.

EXPERIMENTAL

λ -Phage DNA

The λ -phage DNA used in this work was purchased from Sigma Chemical Co. The molecular weight of the DNA was 3.1×10^7 Da, which corresponds to 48,502 base pairs. The molecular weight distribution was monodisperse, which was assessed using agarose gel electrophoresis (Fig. 1, lane A). Lyophilized DNA powder was dissolved into 0.2M of NaCl aqueous solution. Sample solutions were (1) 10 $\mu\text{g}/\text{mL}$ of DNA, 0.24M of NaCl, and 80% glycerol; (2) 7 $\mu\text{g}/\text{mL}$ of DNA, 0.24M of NaCl, and 80% glycerol; and (3) 5 $\mu\text{g}/\text{mL}$ of DNA, 0.24M of NaCl, and 80% glycerol. Glycerol was used as a viscosity builder. λ -Phage DNA molecules have been reported to have a radius of gyration R_g of about 1 μm in an aqueous solution.¹ This R_g value suggests that the c^* for the dilute solution of this polymer should be 12 $\mu\text{g}/\text{mL}$. The concentration of all of sample solutions used was below c^* .

Apparatus

The elongational flow field was generated by a four-roller mill system which has been described in detail previously.¹¹ To record the birefringence pattern microscopically, a Panasonic portable video cassette recorder NV-180 and a Panasonic video camera Model WVP-F2EB were used. Birefringence was calculated by taking the square root of the intensity which was obtained by a photodiode.

The results of the measurements using glass equipment coated with a thin silicon rubber layer were compared with the results of measurements without the silicon coating. Both results were the same, even quantitatively. In the following, we present the results of both sets of measurements. All the measurements were performed at room temperature.

RESULTS AND DISCUSSION

It has been known that DNA molecules of a high molecular weight are easily degraded by shear flow fields. However, the critical fracture strain rate $\dot{\epsilon}_f$ for λ -phage DNA ($M_w = 3.1 \times 10^7$ Da) solution without the viscosity builder was found to be ~ 5

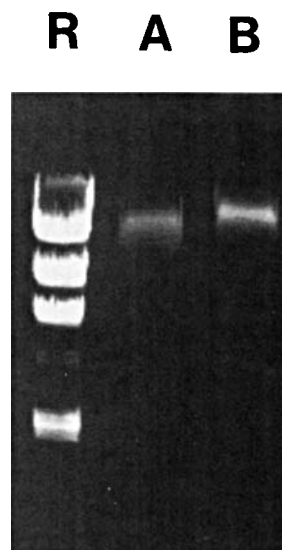


Figure 1 Agarose gel electrophoresis of λ -phage DNA before (lane A) and after (lane B) the elongational flow experiments. Lane R shows the reference bands.

$\times 10^3 \text{ s}^{-1}$.⁹ In this work, elongational flow experiments were carried out for strain rates $\dot{\epsilon} < 50 \text{ s}^{-1}$. Before and after the elongational flow experiments, the molecular weight of DNA was checked by electrophoresis and it was confirmed that the molecular weight did not decrease (Fig. 1, before [lane A] and after [lane B] the experiment). Therefore, there was no need for us to consider flow-induced molecular scission.

Glycerol is known to be a denaturant for the DNA double helix.¹² However, the existence of more than 0.2M of NaCl maintains the duplex conformation of DNA even in a solution with 80% glycerol, which was proved by UV absorption spectrum assessment of the sample solutions containing 80% glycerol and 0.24M of NaCl.

Pattern Observation

At $\dot{\epsilon} = 24 \text{ s}^{-1}$, when the crossed polarizer and analyzer are positioned at 45° to the mill inlet and outlet direction, birefringence was observed all over the area enclosed by the rollers for all the DNA concentrations examined. Intensity along the exit symmetry plane was larger than that in the off-symmetry plane. A small rotation of the compensator showed that the direction of the optical axis in the brightest birefringence is slightly different from that in the birefringence in the off-symmetry plane. Figure 2 shows the birefringence profile along the inlet symmetry plane at eight stages in the experimental range of applied strain rates. These were obtained by mea-

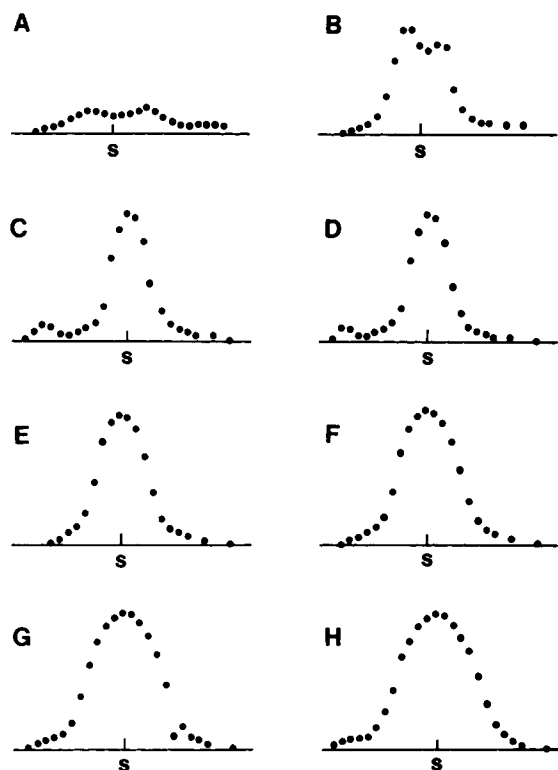


Figure 2 Birefringence profile for 10 $\mu\text{g/mL}$ of λ -phage DNA solution along the inlet symmetry axis at eight stages from $\dot{\epsilon} = 2 \text{ s}^{-1}$ to 24 s^{-1} : (A) 2 s^{-1} ; (B) 3 s^{-1} ; (C) 4 s^{-1} ; (D) 5 s^{-1} ; (E) 7 s^{-1} ; (F) 10 s^{-1} ; (G) 16 s^{-1} ; (H) 24 s^{-1} .

asuring the intensity profile from “stills” at fixed strain rates from the video recording and plotting the birefringence on an arbitrary scale. It was found that

1. Nonlocalized birefringence appears first.
2. A sharp localized birefringence line then appears.
3. The localized line thickens.

Preliminary experiments for a solution of $7 \mu\text{g/mL}$ concentration of DNA shows that the half-width of the birefringence profile does not change with the DNA concentration. The birefringence intensity changes continuously from the outermost part on the inlet line to a point in the vicinity of the stagnation point.

When the polarizer and analyzer directions were placed parallel and perpendicular to the entry and exit directions, respectively, a birefringent signal was not observed at all. According to accumulated results for elongational flow experiments of polymers,¹³ this result indicates that the optical axis of the birefringent solution is almost parallel to the exit symmetrical axis.

Intensity Measurements

All the intensity measurements were carried out with a polarizer and analyzer inclined at 45° to the mill inlet and outlet directions. Figure 3 shows the flow birefringence, Δn , plotted against the strain rate, $\dot{\epsilon}$, for (\circ) $10 \mu\text{g/mL}$, (\bullet) $7 \mu\text{g/mL}$, and (Δ) $5 \mu\text{g/mL}$ solutions of DNA. It can be seen that there is a critical strain rate, $\dot{\epsilon}_c$. Up to $\dot{\epsilon}_c$, $\Delta n = 0$; from $\dot{\epsilon}_c \sim 1 \text{ s}^{-1}$ to $\dot{\epsilon} \sim 3 \text{ s}^{-1}$, Δn increases rapidly; and for $\dot{\epsilon} > 3 \text{ s}^{-1}$, Δn gradually increases.

Free-draining Nature of DNA Coil

Odell and Taylor regarded the criticality at $\dot{\epsilon}_c$ as the manifestation of the coil-stretch transition of “DNA coils.”¹⁰ They reported that the change in the chain hydrodynamic property from nonfree draining to free draining reduces the criticality of the transition. The birefringence pattern with the birefringence intensity profile along the mill inlet symmetry axis observed here also evidences the reduced criticality of the transition and then the free-draining nature of the DNA coil in the solution.

When a polymer molecule, whose monomer unit is birefringent in nature, is a free-draining chain,

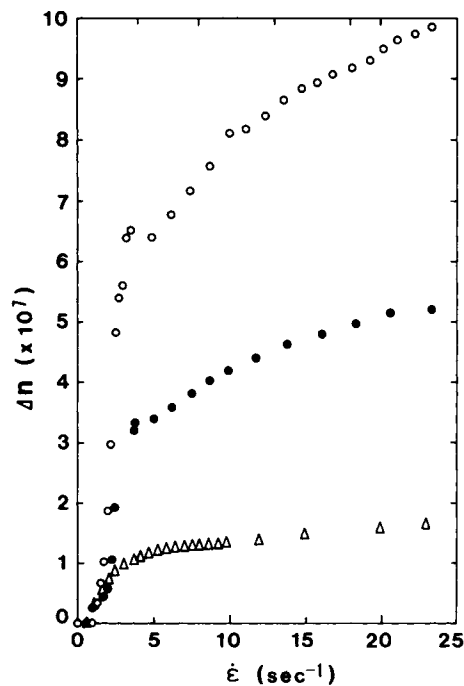


Figure 3 Elongational flow-induced birefringence intensity, Δn , plotted against strain rate, $\dot{\epsilon}$, for (\circ) $10 \mu\text{g/mL}$, (\bullet) $7 \mu\text{g/mL}$, and (Δ) $5 \mu\text{g/mL}$ of λ -phage DNA solutions.

molecular deformation tends to occur at any strain rate. Then, in the Δn vs $\dot{\epsilon}$ plot, the criticality for the coil-stretch transition is reduced, and in the birefringent pattern, the boundary of the localization become ambiguous. This is exactly the situation for λ -phage DNA coils (Figs. 2 and 3). In this case, the birefringence observed is attributed to the deformation of the molecular coil.

Relaxation Process

Observation of Δn decay after a cessation of the flow provides information about the dynamic properties of molecules. However, purely operational considerations restrict the range and accuracy of results based upon a cessation of flow in the four-roll mill. In the case of the equipment used in this work, it takes no more than $\frac{1}{30}$ s (the time for recording one frame of a video) for the flow of the fluid to stop because of a suitable strain rate at the cessation.

Figure 4 shows the relaxation process of Δn after the sudden stop of the flow at 24 s^{-1} for $10 \mu\text{g/mL}$ of the DNA solution. For all the solutions measured, there were two distinct processes: an initial rapid relaxation (stage 1) followed by a slow relaxation (stage 2). The result was obtained by a photodiode and the measured birefringence was integrated all over the microscopic field. There was, however, a distribution of Δn in the field as shown in Figure 2. Figure 5 shows the time evolution of the birefringence profile for $10 \mu\text{g/mL}$ of the DNA solution, after the mill is stopped at the strain rate of 24 s^{-1} , along the inlet symmetry plane. It is clearly shown that the birefringence at the off-symmetrical plane or foot region in the profile decreases faster than that near the stagnation point. Figure 6(a) shows Δn decay after the stopping of the mill at each point of the inside area of the four rollers (at each point in the profiles in Fig. 5), where $\log \Delta n$ are plotted

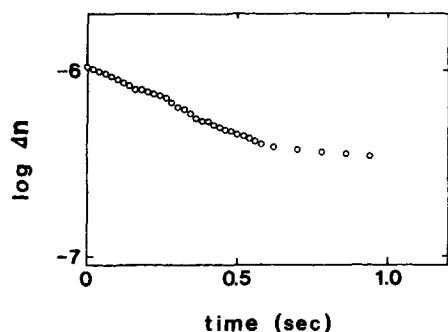


Figure 4 A typical decay curve of flow-induced birefringence for $10 \mu\text{g/mL}$ of DNA solution after the cessation of the flow at the strain rate $\dot{\epsilon} = 24 \text{ s}^{-1}$.

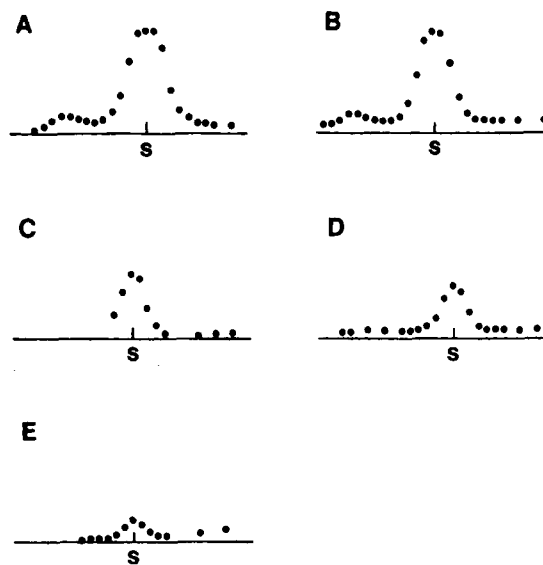


Figure 5 The time evolution of the birefringence profile for $10 \mu\text{g/mL}$ of DNA solution, after the mill is stopped, along the inlet symmetry plane for (A) $t = 0.2 \text{ s}$, (B) 0.3 s , (C) 0.5 s , (D) 0.8 s , and (E) 1 s .

against the frame number which is proportional to the time after the cessation of the mill. In every plot, $\log \Delta n$ is linearly related to time. (In the decay at 2.5 mm from the stagnation point, only the initial part shows the linear relation. The deviation from the relation was due to the uncertainty of the background Δn value.) This linearity indicates that during the observation at least the relaxation is caused by a single mechanism of molecular relaxation. The slope of the decay increases with the distance from the central stagnation point. Figure 6(b) shows the relative relaxation time, τ_r , at each point in the flow field where the values are normalized by the value at the stagnation point. It was found that the τ_r of a molecule which has just entered the mill is small and τ_r increases as it approaches the stagnation point. A still such as in Figure 2 is the integrated record over $\frac{1}{30}$ s. The last frame in Figure 6 was recorded at about 0.4 s after the mill stopped. From a comparison of Figure 4 with Figure 6(a), stage 1 in Figure 4 can be attributed to an observation of a parallel multirelaxation process in the mill space. Stage 2 was considered to be a prolonged birefringence relaxation near the stagnation point.

In the stopped flow measurements, the relaxation process of the flow birefringence is generally regarded as containing both a disorienting process of deformed molecules and a recovering process from the deformed conformation. Both stage 1 and stage 2 are thought to be based on a single mechanism, since in both processes, the relaxation proceeds as

a simple exponential function. The largest relaxation time in stage 1 was 0.52 s and the relaxation time of stage 2 was 6.7 s, where the latter value is similar to the longest molecular relaxation time for the λ -phage DNA: 3 s for a molecule of 12.8 μm .¹ From this fact, we conclude that the main contributor to stage 2 is the molecular recovering process, and the dominant mechanism of stage 1 is a disorientation process of deformed molecules.

Degree of Molecular Deformation

As we concluded that stage 1 is dominated by the disorientation process of deformed molecules, observed relaxation time, τ , is related to the rotational diffusion coefficient, D_r ; $\tau = \frac{1}{6}D_r$. D_r is generally related to a parameter characterizing an anisotropic structure of a molecule such as an aspect ratio, p . In the elongational flow field generated by the four-roller mill, a molecular coil is considered to be deformed in a prolate spheroid. For a prolate spheroid, the relation is described as¹⁴

$$D_r = (3kT/16\pi ab^2\eta_s)[p^2/(1-p^4)]\{[(2-p^2)/2(1-p^2)^{1/2}]\ln\{[1+(1-p^2)^{1/2}]/[1-(1-p^2)^{1/2}]\}-1\} \quad (1)$$

where k is the Boltzmann constant; T , the absolute temperature; a and b , respectively, the longer and shorter radii of the prolate spheroid ($p = b/a \leq 1$); and η_s , the viscosity of the solvent. The ratio of D_r of the molecule at the outer most region (just when it enters the mill space), D_0 , to that at the stagnation point, D_s , ($D_0/D_s = A$), is described as

$$(A/a_s^3)[f(p_s)/p_s^2] = (1/a_0^3)[f(p_0)/p_0^2] \quad (2)$$

where

$$f(p) = [p^2/(1-p^4)]\{[(2-p^2)/2(1-p^2)^{1/2}]\ln\{[1+(1-p^2)^{1/2}]/[1-(1-p^2)^{1/2}]\}-1\}. \quad (3)$$

Assuming for the DNA coil,

$$4\pi a_s^3 p_s^2/3 = 4\pi a_0^3 p_0^2/3 \quad (4)$$

hence,

$$Af(p_s) = f(p_0) \quad (5)$$

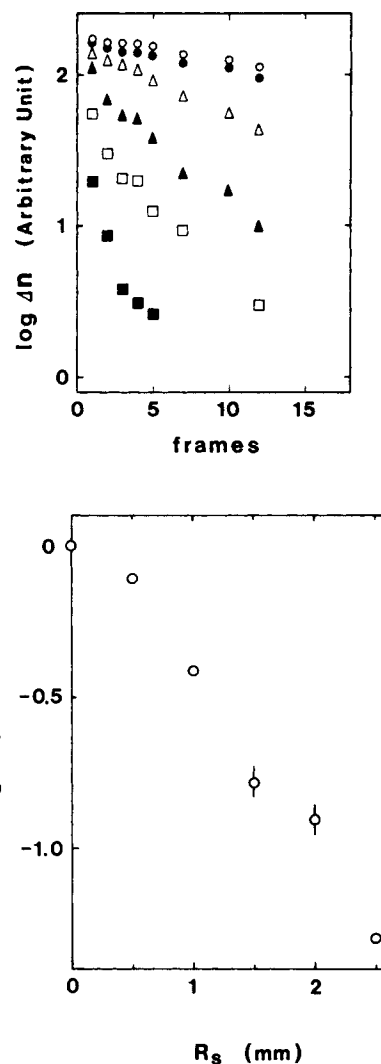


Figure 6 (a) Logarithm of Δn plotted against time (in video frame units; one frame corresponds to $\frac{1}{30}$ s) on the inlet symmetry plan at (○) the stagnation point, (●) 0.5 mm, (△) 1.0 mm, (▲) 1.5 mm, (□) 2.0 mm, and (■) 2.5 mm from the stagnation point for 10 $\mu\text{g}/\text{mL}$ solution. (b) Relative relaxation time τ_r , plotted against the distance from the stagnation point, R_s . The relaxation time at each point was normalized by the value at the stagnation point.

Figure 7 shows the plot of $f(p)$ as a function of p . $f(p)$ is found to be a decreasing function of p . According to Figure 6(b), A is 20. A molecule which has just entered the mill space has an aspect ratio slightly smaller than 1, because the molecule manifested the birefringence. If we assume $p_0 \sim 0.95$, $f(p_0) \sim 0.66$, and, thereby, $f(p_s) \sim 0.033$, then, $p_s \sim 0.08$. Menasveta and Hoagland reported that the change in R_g by the coil-stretch transition in polystyrene was at the most a factor of 2,⁷ from 350 nm in the coiled state to 650 nm in the stretched state

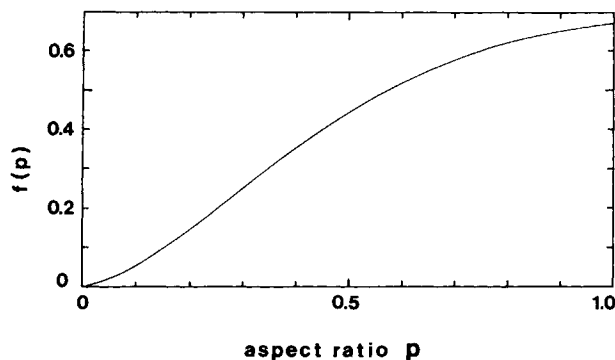


Figure 7 $f(p)$ in eq. (3) plotted against the aspect ratio, p , of the prolate spheroid.

in an elongational flow field at a strain rate of more than 10^3 s^{-1} . This duplication in the R_g value corresponds to a decrease in p to $\frac{1}{6}$ of the p value of the coil.⁸ Our value of $p_s/p_0 \sim \frac{1}{12}$ is smaller than the value reported by Menasveta and Hoagland for polystyrene. The strain rate for the extension of molecules in our experiment is 24 s^{-1} and this is far smaller than the value $\sim 10^3 \text{ s}^{-1}$, around which the coil-stretch transition for polystyrene was observed.⁷ In the case of λ -phage DNA, the coil-stretch transition seems to be still proceeding at 24 s^{-1} , which suggests that the DNA coil will be continually elongated over this strain rate.

CONCLUSIONS

The birefringence pattern in the mill space (Fig. 2) and the shape of the Δn vs. $\dot{\epsilon}$ plot (Fig. 3) indicate the reduced criticality of the coil-stretch transition of "DNA coils" in the elongational flow field. The reduced criticality suggests that the DNA molecule in the solution is regarded as a free-draining coil. At the strain rate of $\dot{\epsilon} = 24 \text{ s}^{-1}$, the aspect ratio p of the DNA molecule as a spheroid is smaller than $\frac{1}{12}$. The free-draining nature suggests that the DNA molecule in the elongational flow field of our experiment is on the way to a more stretched conformation. There is a possibility that the DNA molecule

is almost in a stretched conformation before scission of the molecule by the elongational flow field begins.

We wish to acknowledge the support of the Venture Research Unit of British Petroleum International. N.S. gratefully acknowledges the financial support by the Saneyoshi Foundation, the CIBA GEIGY Foundation, and a Grant-in-Aid for Scientific Research (No. 05650910) from the Ministry of Education, Culture and Science, Japan.

REFERENCES

1. T. T. Perkins, D. E. Smith, and S. Chu, *Science*, **264**, 819–822 (1994).
2. K. Minagawa, Y. Matsuzawa, K. Yoshikawa, A. R. Khokhlov, and M. Doi, *Biopolymers*, **34**, 555–558 (1994).
3. P. G. De Gennes, *J. Chem. Phys.*, **60**(12), 5030–5042 (1974).
4. D. G. Crowley, F. C. Frank, M. R. Mackley, and R. G. Stephenson, *J. Polym. Sci. Polym. Phys. Ed.*, **14**, 1111–1119 (1976).
5. A. Keller and J. A. Odell, *Colloid Polym. Sci.*, **263**, 181–201 (1985).
6. J. A. Odell, A. J. Muller, K. A. Narh, and A. Keller, *Macromolecules*, **23**, 3092–3103 (1990).
7. M. J. Menasveta and D. A. Hoagland, *Macromolecules*, **24**, 3427–3433 (1991).
8. *International Tables for X-Ray Crystallography*, C. H. Macgillavry and G. D. Rieck, Eds., Kynoch Press, Birmingham, 1962, Vol. 3, p. 327.
9. E. D. T. Atkins and M. A. Taylor, *Biopolymers*, **32**, 911–923 (1992).
10. J. A. Odell and M. A. Taylor, *Biopolymers*, **34**, 1483–1493 (1994).
11. N. Sasaki, E. D. T. Atkins, and S. W. Fulton, *J. Appl. Polym. Sci.*, **42**, 2975–2985 (1991).
12. E. L. Duggan, S. L. Bunch, S. L. Louie, and A. N. Brown, *Biochem. Biophys. Res. Commun.*, **6**(2), 93–99 (1961).
13. J. A. Odell, A. Keller, and E. D. T. Atkins, *Macromolecules*, **18**(7), 1443–1453 (1985).
14. M. Doi and S. F. Edwards, *The Theory of Polymer Dynamics*, Clarendon Press, Oxford, 1986, Chap. 8.

Received March 1, 1995

Accepted August 11, 1995